1

TRANSPORT OF POLLUTANTS

1.1 INTRODUCTION

Pollutants are dispersed in aquatic systems through advection and mixing. Although mixing occurs at the molecular level and by eddy diffusion, it is the eddy diffusion which is of primary interest in actual systems. Mixing is important for the effective dispersal of pollutants from a wastewater outfall into a lake, coastal zone, or estuary. Dispersal is aided by a high exit velocity, currents in the coastal zone, or river flow velocity. Horizontal mixing in lakes can be impeded by the development of thermal fronts, which are particularly prevalent during the spring warming period in nearshore areas lakes (Christensen et al., 1997). The thermal front is formed when lake water that is cooled below 4°C meets nearshore water that has been warmed to a higher temperature to form a vertical barrier of 4°C water. This barrier moves out into the lake and becomes less distinctive as spring warming progresses.

In most lakes and nearshore areas, thermal stratification will develop during the summer, and this effectively isolates the warm epilimnion, or upper layer, from the cold hypolimnion or bottom layer. The intensity of vertical mixing can be inferred from density gradients or by measurement of ^{222}Rn or the tritium–helium-3 pair.

Other phenomena such as up and down welling and inertial Kelvin waves (Wetzel, 1975) can influence water currents and temperatures, which is reflected in the temperature records of water intakes for the Great Lakes. For coastal areas, tides can be of great significance in creating nearshore currents. In the Bay of Fundy on the US east coast, the fjord configuration acts to amplify the difference in water levels between ebb and flood to a total of 18–22 m. While many ocean wastewater outfalls are beyond the direct influence of these currents, they have the potential to

Physical and Chemical Processes in the Aquatic Environment, First Edition. Erik R. Christensen and An Li.

disperse pollutants during ebb, but also to exacerbate pollutant impact on coastal areas during flood.

Pollutant plumes of groundwater can occur as a result of BTEX (benzene, toluene, ethylbenzene, and xylene) compounds leaking from underground storage tanks (Frieseke and Christensen, 1995) or from low molecular weight organics used in dry-cleaning operations. Nitrates from fertilizers can also create significant groundwater pollution (Lee et al., 1995). For groundwater, the dispersion coefficient is proportional to the pore velocity, and plume retardation may occur as a result of partitioning to the solid organic phase.

Dissolved organic carbon (DOC), such as humic acid, can increase the rate of transfer of hydrophobic chemicals such as PCBs (polychlorinated biphenyls) and PBDEs (polybrominated diphenyl ethers) between the aqueous and sorbent phases (ter Laak et al., 2009). The DOC–water partition coefficient K_{DOC} (l/kg) increases with planarity of PCBs, apparently reflecting increased sorption for PCBs with one or no *ortho*-substituted carbon atoms. The facilitated transport can be important for uptake by organisms or passive samplers when equilibration is slow or occurs under time-varying conditions.

Mixing in aquatic sediments is of interest both for the distortion it can impart on historical records of particle-bound pollutants (Christensen and Karls, 1996) and because of the increased chance of pollutant release from the sediment to the water column of in-place pollutants (Christensen et al., 1993). The formulation of the advection–diffusion equation depends on whether or not the tracer (pollutant) is associated with settling particles or colloids (Fukumori et al., 1992).

1.2 ADVECTION–DIFFUSION EQUATION WITH REACTION

The general form of the 3-D advection–diffusion equation for aquatic systems is,

$$\frac{\partial c}{\partial t} + \frac{\partial uc}{\partial x} + \frac{\partial vc}{\partial y} + \frac{\partial wc}{\partial z} = \frac{\partial}{\partial x}\left(D_x \frac{\partial c}{\partial x}\right) + \frac{\partial}{\partial y}\left(D_y \frac{\partial c}{\partial y}\right) + \frac{\partial}{\partial z}\left(D_z \frac{\partial c}{\partial z}\right) + R \quad (1.1)$$

where

c = concentration of a species,
t = time,
u, v, w = water velocities in the x, y, and z directions, respectively,
D_x, D_y, D_z = eddy diffusion coefficients in the x, y, and z directions, respectively, and,
R = production rate of the species per unit volume.

The molecular diffusivity in water is 2×10^{-5} cm^2/s (Weber and DiGiano, 1996). For oceans and lakes, the horizontal eddy diffusivities D_x and D_y are in the range of 10^4–10^8 cm^2/s, and the vertical diffusivity D_z is between 10^1 and 10^3 cm^2/s.

The water velocities u, v, and w are either measured or may be obtained from the momentum conservation equation, i.e., the Navier–Stokes equation (Weber and

DiGiano, 1996). In the case of groundwater, this equation is reduced to the Darcy equation, which states that the average groundwater velocity is proportional to the gradient of the hydraulic head. For sediments, the velocity relative to the sediment–water interface is derived by dividing the mass sedimentation rate by the bulk sediment density ρ, where ρ can be modeled based on soil mechanics concepts (Fukumori et al., 1992).

As will be shown below, simple versions of Equation 1.1, especially one-dimensional cases, can be solved analytically. More realistic configurations can be addressed by finite differences or finite elements techniques.

A version of the one-dimensional advection–diffusion equation for solute transport, including advection, dispersion, and transient storage, was considered by Cox and Runkel (2008). The authors included both fixed grid (Eulerian) and traveling control volumes (Lagrangian). The Lagrangian approach has the advantage that advection is zero; therefore the mass losses that are often seen in Eulerian approaches are eliminated. However, the Lagrangian method has the numerical inconvenience of non-fixed and possibly deforming grids. The mass losses and oscillation and dispersion problems experienced in the Eulerian approach can be eliminated by reducing the grid Peclet numbers ($P = U\Delta x/D$) and Courant numbers ($\mathrm{CN} = U\Delta t/\Delta x$) at the expense of increased computation time. Here U is flow velocity, Δt is time step, Δx is the grid size, and D is the dispersion coefficient. Cox and Runkel proposed a combined approach in which the grid is fixed through interpolation and back-tracking of moving cell flow paths.

Another example of the application of Equation 1.1 is shown by Li et al. (2008), where the one-dimensional advection equation, modified with a solid phase attachment term, was used to model transport and deposition of fullerene (C_{60}) nanoparticles in water-saturated porous media. These particles currently have several applications in, for example, biomedical technology and cosmetics, and, because of their toxicity to aquatic biota and human cells, an understanding of the fate and transport of these nanoparticles is important. They have negligible solubility in water but can form stable nanoscale aggregates ($n\mathrm{C}_{60}$) by acquiring negative surface charge. Li et al. (2008) found that clean-bed filtration theory, modified to consider shadow zones and surface charge heterogeneity, could be used to predict ($n\mathrm{C}_{60}$) transport in saturated porous media.

While the emphasis in this chapter is on the quantitative prediction of pollutant transport by means of equations such as Equation 1.1, one should realize that tracers can play an important role in the estimation of fate and transport of pollutants. An example of this is the use of stable ^{127}I and radioactive ^{129}I to evaluate the dispersion of ^{129}I from the French nuclear reprocessing facility in La Haque (Hou et al., 2007). From measurements of ^{127}I and ^{128}I in the English Channel and the North Sea it was found that the influence of the La Haque facility on ^{129}I distribution is clearly reflected in surface water of the North Sea. It was also concluded that reduction of iodate (IO_3^-) to iodide (I^-) in ^{129}I is a relatively fast reaction during transport to the European continental coast, while oxidation of I^- to IO_3^- is low between coastal areas and the open sea. The application of tracers to pollution plumes will be further explored in Chapter 9.

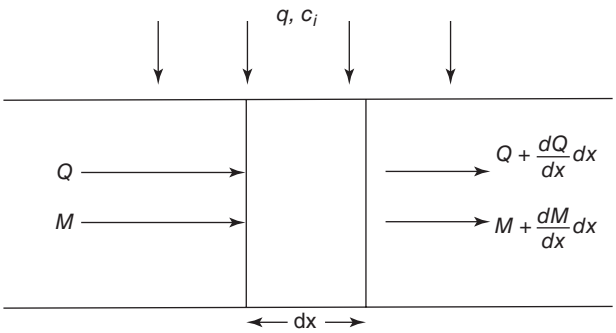

Figure 1.1. Definition sketch for a one-dimensional advection–diffusion equation with reaction.

1.3 STEADY-STATE MIXING IN ESTUARIES

Consider the simplified sketch of a stretch of an estuary or river in Figure 1.1.

Mass balance equations for water and pollutant of concentration c may be written as:

$$\text{Inflow} + \text{Discharge} = \text{Outflow},$$

or,

$$\left.\begin{aligned} Q + qdx &= Q + (dQ/dx)\,dx \\ M + qc_i dx &= M + (dM/dx)dx \end{aligned}\right\} \tag{1.2}$$

where

Q = water flow m^3/s,
q = discharge per unit length $\mathrm{m}^3/(\mathrm{m\ s})$
M = pollutant mass flow kg/s
c_i = concentration of pollutant in the discharge kg/m^3.

From Equation 1.2 we obtain,

$$\left.\begin{aligned} \frac{dQ}{dx} &= q \\ \frac{dM}{dx} &= qc_i \end{aligned}\right\} \tag{1.3}$$

From Fick's law, the pollutant mass flow M may be expressed as,

$$M = Qc - AD\frac{dc}{dx} \tag{1.4}$$

where A (m^2) is the cross sectional area of the estuary and D (m^2/s) is the diffusion (dispersion) coefficient of diffusivity. If A and D are independent of x we obtain from

Equations 1.3 and 1.4,

$$\frac{Q}{A}\frac{dc}{dx} - D\frac{d^2c}{dx^2} = \frac{q}{A}(c_i - c) \tag{1.5}$$

In the case where $c_i \gg c$ the second term on the right hand side drops out. This result could also have been obtained directly from the 3-D advection–diffusion equation, Equation 1.1.

1.3.1 Determination of Diffusivity *D* from Salinity Measurements

Diffusivity D may be estimated from measurements of salinity in an estuary (Harremoës, 1978), or from conductivity in a freshwater estuary such as the Fox River, Wisconsin, United States, which empties into Green Bay. For an infinitely long estuary (Figure 1.2a), the net flow of salinity M at any value x must be zero under steady-state conditions. Thus, from Equation 1.4,

$$c = c_0 \mathrm{e}^{\frac{Q}{AD}x} \tag{1.6}$$

where c_0 is the ocean salinity. If the measured value of the salinity is c_x at the position x, the diffusivity D may be calculated from Equation 1.6,

$$D = \frac{Qx}{A}\frac{1}{\ln\frac{c_x}{c_0}} \tag{1.7}$$

For the case of a uniform estuary with even discharge (Figure 1.2b), we obtain,

$$\frac{dc}{dx} = \frac{Q}{AD}c = \frac{qx}{AD}c \tag{1.8}$$

When this is inserted into Equation 1.4 with $M = 0$ we obtain,

$$c = c_L \mathrm{e}^{\frac{q}{2AD}(x^2 - L^2)} \tag{1.9}$$

where c_L is the ocean salinity and L is the estuary. One example of a solution for c is shown in Figure 1.2b. Thus if the salinity is measured to be c_0 for $x = 0$, and diffusivity D can be expressed as,

$$D = \frac{qL^2}{2A\ln\frac{c_L}{c_0}} \tag{1.10}$$

1.3.2 Pollutant Prediction for an Estuary with Uniform Discharge

For a conservative, the net mass transfer across a boundary at x under steady-state conditions (Figure 1.3) is equal to the mass discharge into the estuary from the left of the boundary,

$$M = qxc - AD\frac{dc}{dx} = qxc_q \tag{1.11}$$

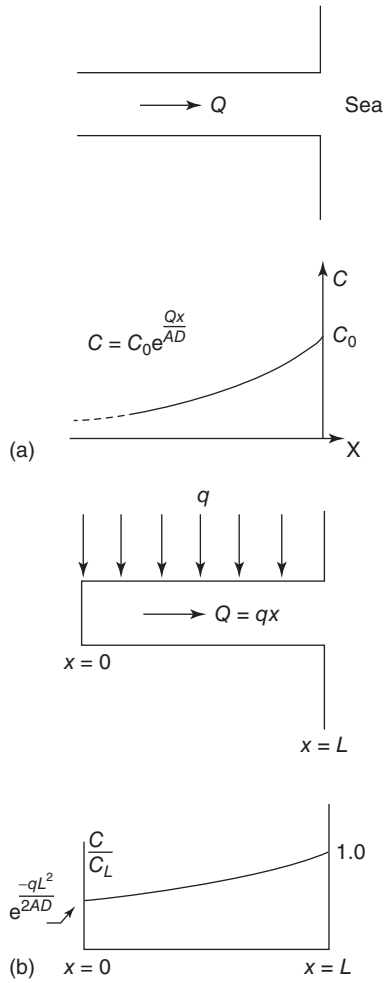

Figure 1.2. Determination of diffusivity D from salinity measurement in (a) an infinitely long estuary, and (b) a uniform estuary with even discharge. (Source: Adapted from Harremoës (1978))

This equation may be integrated to give,

$$\frac{c - c_q}{c_L - c_q} = e^{-\frac{qL^2}{2AD}\left(1-\left(\frac{x}{L}\right)^2\right)} \tag{1.12}$$

where c_q is the pollutant concentration in runoff and c_L is the pollutant concentration at the mouth of the estuary. Pollutant concentrations according to this equation are plotted for both $c_L > c_q$ and $c_L < c_q$ in Figure 1.3.

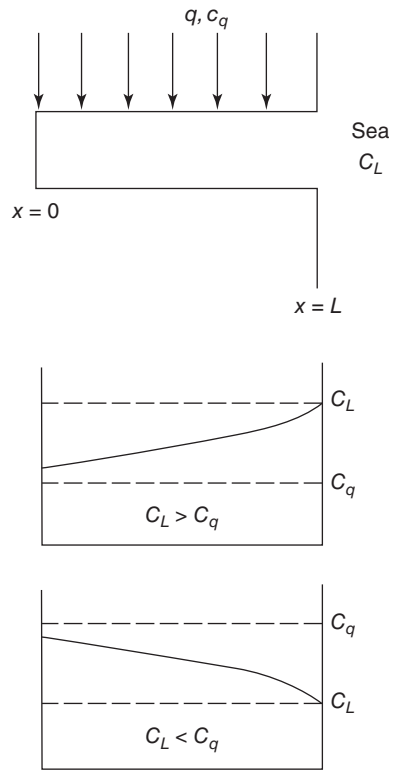

Figure 1.3. Conservative pollutants prediction in uniform estuary with even discharge. (Source: Adapted from Harremoës (1978))

In the case where the pollutant is non-conservative, e.g. nitrogen lost by de-nitrification processes to the sediments, Equation 1.11 may be modified as follows:

$$M = qxc - AD\frac{dc}{dx} = qxc_q - Wxr_a \tag{1.13}$$

where W is the width (m) of the estuary and r_a (kg/(m^2 s)) is a zero order removal rate. The solution to this equation is

$$\frac{c - \left(c_q - \dfrac{Wr_a}{q}\right)}{c_L - \left(c_q - \dfrac{Wr_a}{q}\right)} = \mathrm{e}^{-\frac{qL^2}{2AD}\left(1-\left(\frac{x}{L}\right)^2\right)} \tag{1.14}$$

In order to determine r_a one may measure the pollutant concentration c at any point in the estuary, and then solve the above equation for r_a.

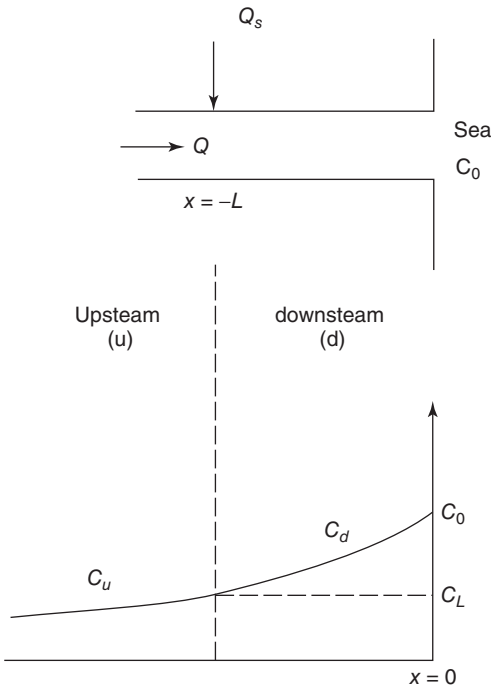

Figure 1.4. Determination of diffusivity D from salinity measurements in an infinite estuary with a large freshwater discharge. (Source: Adapted from Harremoës (1978))

1.3.3 Salinity in an Infinite Estuary with a Large Freshwater Discharge

The case of an infinitely long estuary with a large freshwater discharge, e.g. from a sewage treatment plant, is considered next (Figure 1.4). The net outflow of salinity into the ocean is still zero both upstream and downstream of the discharge point ($x = -L$):

$$\text{Upstream,} \qquad M = Qc - AD\frac{dc}{dx} = 0 \tag{1.15}$$

$$\text{Downstream,} \qquad M = (Q + Q_s)c - AD\frac{dc}{dx} = 0 \tag{1.16}$$

where Q_s (m^3/s) is the freshwater discharge from the point source. Equations 1.15 and 1.16 are solved using the following boundary conditions:

$$\left.\begin{array}{ll} x = 0 & c_d = c_0 \\ x = -L & c_u = c_d = c_L \\ x \to -\infty & c_u \to 0 \end{array}\right\} \tag{1.17}$$

where c_d and c_u are the downstream and upstream solutions, respectively. The solution can be expressed as,

$$\frac{c_u}{c_L} = \mathrm{e}^{\frac{Q}{AD}(x+L)} \tag{1.18a}$$

$$\frac{c_d}{c_0} = \mathrm{e}^{\frac{Q+Q_s}{AD}x} \tag{1.18b}$$

A sketch of this solution is shown in Figure 1.4. From Equation 1.18b we obtain with $c_d = c_L$ for $x = -L$:

$$D = \frac{Q+Q_s}{A} L \frac{1}{\ln \frac{c_0}{c_L}} \tag{1.19}$$

Therefore, diffusivity D can be calculated based on the measured salinity c_L at $x = -L$.

1.3.4 Conservative Pollutant Prediction for an Infinite Estuary with a Large Freshwater Discharge

With the diffusivity calculated from salinity as a natural tracer, e.g. according to Equation 1.19, it is now possible to predict the distribution of a conservative pollutant that is discharged from the point source with the concentration c_s (Figure 1.5). The net mass transfer of the pollutant of concentration c in the upstream area at any value of x is zero for steady-state conditions,

$$M = Qc - AD\frac{dc}{dx} = 0 \tag{1.20}$$

However, for the downstream section, the mass transfer at any boundary must equal the pollutant mass discharged from the point source,

$$M = Qc - AD\frac{dc}{dx} = Q_s c_s. \tag{1.21}$$

The upstream and downstream solutions to Equations 1.20 and 1.21 with the same boundary conditions as for the salinity distribution, Equation 1.17, can be expressed as,

$$c_d = \frac{Q_s}{Q+Q_s}c_s + \left[c_0 - \frac{Q_s}{Q+Q_s}c_s\right] * \mathrm{e}^{\frac{Q+Q_s}{AD}x} \tag{1.22}$$

$$c_u = \left[\frac{Q_s}{Q+Q_s}c_s + \left(c_0 - \frac{Q_s}{Q+Q_s}c_s\right)\mathrm{e}^{-\frac{Q+Q_s}{AD}L}\right] * \mathrm{e}^{\frac{Q}{AD}(x+L)} \tag{1.23}$$

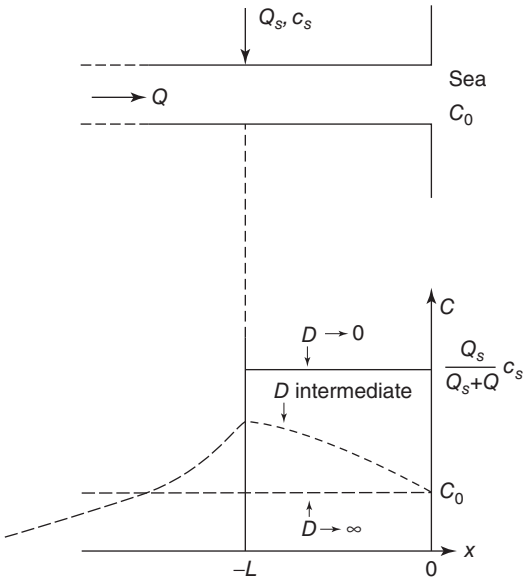

Figure 1.5. Conservative pollutants prediction in infinite estuary with a large freshwater discharge. (Source: Adapted from Harremoës (1978))

The above solutions are indicated in Figure 1.5 along with the limiting cases of $D \to \infty$ corresponding to vigorous mixing ($c = c_0$), and $D \to 0$ reflecting little mixing. In the latter case, the pollutant concentration is given by

$$c = \frac{Q_s}{Q + Q_s} c_s \tag{1.24}$$

in the downstream area ($x > -L$) and $c = 0$ upstream ($x < -L$). In the downstream area, this is, of course, the same as would be obtained by simple dilution of the effluent with the estuary flow. The actual pollutant concentration falls between those of the limiting cases in the downstream area, and is also noticeable (> 0) upstream of the discharge point (Figure 1.5).

1.4 TIME-DEPENDENT MIXING IN RIVERS AND SOIL SYSTEMS

The one-dimensional (1-D) advection–diffusion equation may be written as,

$$-v\frac{\partial c}{\partial x} + D\frac{\partial^2 c}{\partial x^2} = \frac{\partial c}{\partial t} \tag{1.25}$$

where the notation is the same as Equation 1.1 except that the velocity in the x-direction v has been named and the subscript for the diffusivity D has been dropped.

Consider the case where a slug of pollutant M (kg/m^2) is released into a river at $x = 0$, $t = 0$. Initially, $c = 0$ everywhere at $t = 0$, except at $x = 0$. The boundary conditions are that $c = 0$ for $x \to \pm\infty$ and that the following condition holds,

$$\frac{M}{v} = \int_0^\infty c(x, \tau) d\tau \tag{1.26}$$

This equation expresses the fact that the total mass per unit area passing through a boundary at x must equal M.

With these conditions, the solution to Equation 1.25 is (Haas and Vamos, 1995):

$$c = \frac{M}{\sqrt{4\pi D t}} \exp\left(-\frac{(x - vt)^2}{4Dt}\right). \tag{1.27}$$

Typical solutions following the release of a conservative pollutant to a river are shown in Figure 1.6. When the diffusion coefficient is low (1.4×10^5 cm^2/s, Figure 1.6a), the peak is sharp and the max value high. As the slug moves downstream, the contaminated area widens and the peak drops. A similar picture is apparent when the diffusivity is higher, except that the bell-shaped curve is more spread out (Figure 1.6b).

From Equation 1.27 we can derive the following relationship,

$$D = \frac{1}{2}\frac{d\sigma^2}{dt}, \tag{1.28}$$

which can be used for an observational or experimental determination of D from the spread over time of a colored or otherwise identifiable pollution patch. This expression was, for example, used in a court case to estimate diffusivity based on the pollution plume in Lake Michigan from a wastewater treatment plant in Milwaukee, Wisconsin (Mortimer, 1981).

To illustrate the application of Equation 1.28, consider Figure 1.6a from which we estimate D as follows:

$$D = \frac{1}{2}\frac{(1.0)^2 - (0.4)^2 \text{ km}^2}{8 \text{ h}} = 0.053\frac{\text{km}^2}{\text{h}}, \tag{1.29}$$

which is close to the actual value of 0.05 km^2/h.

The horizontal diffusivity in the flow direction of a river may also be estimated from the equation (McQuivey and Keefer, 1974):

$$D = 0.058\frac{Q_0}{S_0 W_0} \tag{1.30}$$

where

Q_0 = volumetric flow rate,
W_0 = width of the river, and
S_0 = slope of the specific energy curve.

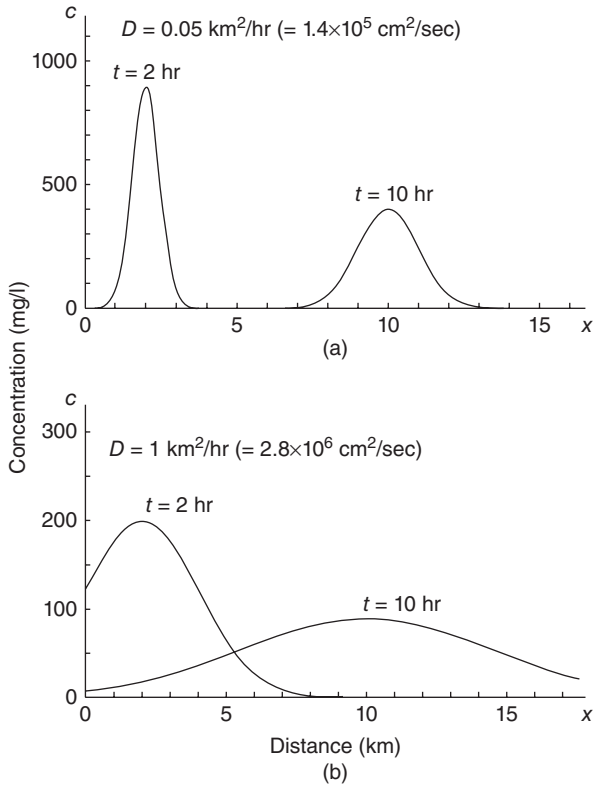

Figure 1.6. Transport and dispersion of a slug of pollutant of $M = 1000$ kg/m^2 in a river with $v = 1$ km/h and (a) $D = 0.05$ km^2/h and (b) $D = 1$ km^2/h.

Rather than an instantaneous release of a slug of a pollutant, a continuous discharge may occur. Consider, for example the continuous leakage of contaminated water into a semi-infinite system such as soil. For such a case, the solution to Equation 1.25 may take one of the following forms (Gershon and Nir, 1969):

$$\frac{c_x}{c_0} = \frac{1}{2}\text{erfc}\left[\frac{x - vt}{2\sqrt{Dt}}\right] + \frac{1}{2}\exp\left(\frac{vx}{D}\right)\text{erfc}\left(\frac{x + vt}{2\sqrt{Dt}}\right) \text{ (SINF1);} \tag{1.31}$$

$$\frac{c_x}{c_0} = \frac{1}{2}\text{erfc}\left[\frac{x - vt}{2\sqrt{Dt}}\right] - \frac{1}{2}\exp\left(\frac{vx}{D}\right)\text{erfc}\left\{\left(\frac{x + vt}{2\sqrt{Dt}}\right) * \left[1 + \frac{v\,(x + vt)}{D}\right]\right\}$$

$$+ v\sqrt{\frac{t}{\pi D}}\exp\left(\frac{vx}{D} - \frac{1}{2}\left(\frac{x + vt}{\sqrt{Dt}}\right)^2\right) \text{ (SINF2);} \tag{1.32}$$

where x is the depth below the surface. The initial condition for both equations is $c(x,t) = c(x,0) = 0$, i.e. no contamination in the soil initially. The exit boundary condition is also the same for the two equations, i.e.

$$\frac{\partial c}{\partial x} \to 0 \text{ for } x \to \infty \text{ all } t$$

However, the two solutions differ with regards to the inlet boundary condition. For Equation 1.31, the inlet condition is,

$$c = c_0 \text{ for } x = 0 \text{ all } t$$

This would be the case in a horizontal column experiment with one end kept at constant concentration. Conversely, a vertical system, e.g. infiltration of leachate into the ground from a landfill is governed by the following flux condition:

$$\left(vc - D\frac{\partial c}{\partial x}\right)_{x=0^+} = J_0 = vc_0 \tag{1.33}$$

This is the inlet boundary condition that applies to Equation 1.32. Note that this is the same type of boundary condition that applies to the influx of a pollutant or tracer into a sediment from the water column (Guinasso and Schink, 1975; Christensen and Bhunia, 1986).

Example solutions, SINF1 and SINF2, according to Equations 1.31 and 1.32 are shown in Figure 1.7. The parameters are here $v = 10$ m/d, $x = 10$ m, and D equal to

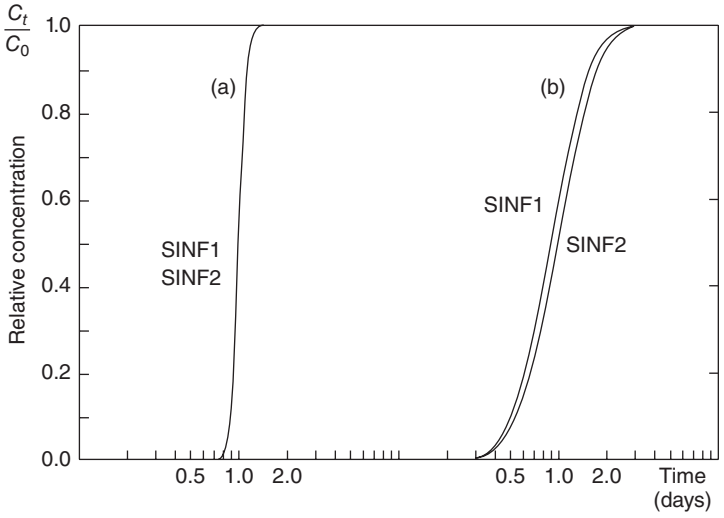

Figure 1.7. Relative concentration vs. time at $x = 10$ m for $v = 10$ m/d and (a) $D = 0.5$ m^2/d and (b) $D = 10$ m^2/d of pollution released at a constant rate for $t \geq 0$ at $x = 0$.

either 0.5 m^2/d (Figure 1.7a) or 10 m^2/d (Figure 1.7b). Note that the front is spread out as D increases. Also, SINF1 is higher than SINF2 when mixing is significant ($D = 10$ m^2/d), and the latter curve, for which the flux inlet condition applies, passes through $c_x/c_0 = 0.5$ for $t = 1$ d. Thus, the flux condition curve progresses into the soil with the velocity $v = 10$ m/d; whereas the mid-point of the concentration condition curve has reached $x = 10$ m in 0.92 days, i.e. travels 9% faster.

Even though velocities, distances, and diffusivities are much lower in the soil infiltration system (Figure 1.7) than in the river (Figure 1.6), the ratio between advective and diffusive transport, i.e. the Peclet number,

$$Pe = \frac{vz}{D} \tag{1.34}$$

is the same in the two cases. Therefore, the time taken to double the concentrations in the soil system may be inferred from the scaled distributions of the river system. The solutions shown in Figure 1.7 were obtained from a table of the error function. An abbreviated version is shown in Table 1.1. For high values of the argument x, the following series expansion was used (Lapidus and Amundson, 1952).

$$\operatorname{erfc}(|x|) = \exp(-x^2)\frac{1}{\sqrt{\pi}}\left[\frac{1}{x} - \frac{1}{2x^3} + \frac{3}{4x^5} - \frac{5}{8x^7} + \cdots\right] \tag{1.35}$$

1.5 VERTICAL MIXING

The vertical diffusivity in a water body may be determined from the ^{222}Rn distribution in the water column, by using the tritium–helium-3 method, or from the vertical density gradient. For lakes, the vertical diffusivity reflects the degree of mixing, which has an impact on the distribution of dissolved oxygen and nutrients. Mixing can make nutrients in the hypolimnion available to bacteria and other organisms in the epilimnion, and the dissolved oxygen levels of the lake will generally increase so as to sustain the fish population and promote aerobic microbial decay.

In a stratified lake nutrients may not be readily available in the epilimnion, and low DO concentrations in the hypolimnion can cause fish deaths. In order to remedy this, artificial de-stratification can be used. Two types are commonly used: a diffuser system with injection of air near the bottom of the lake (Schladow and Fisher, 1995), and an axial flow system, with impellers placed below the water surface, moving warm, well-aerated lake water downward (Lawson and Anderson, 2007).

An axial flow system for de-stratification and mixing in Lake Elsinore, California, was investigated by Lawson and Anderson (2007). The lake is relatively shallow with typical depths from 3 to 7 m. It is polymictic, i.e. too shallow to develop stable thermal stratification. The axial pumps had little effect on stratification and DO levels in the lake. Measurement from an Acoustic Doppler current profiler showed inefficient lateral transmission of mixing energy into the water column. This was probably due to excessive turbulence near the axial pumps, the shallowness of the lake, and the

TABLE 1.1. Selected Values of erf(x)

x	0	1	2	3	4	5	6	7	8	9
0	0	0.11246	0.22270	0.32863	0.42839	0.52050	0.60386	0.67780	0.74210	0.79691
1	0.84270	0.88021	0.91031	0.93491	0.95229	0.96611	0.97635	0.98379	0.98909	0.99279
2	0.99532	0.99702	0.99814	0.99886	0.99931	0.99959	0.99976	0.99987	0.99992	0.99996

Note $\mathrm{erfc}(x) = 1 - \mathrm{erf}(x)$
$\mathrm{erf}(x) = -\mathrm{erf}(x)$

relatively flat lake bottom. Winter storms in 2005 had a larger effect on water column parameters than the axial pumps.

A shallow mixing depth can be of concern for drinking water supplies as a result of the potential for excessive algal growth, as recently documented for tributary bays of the Yangtze River near the Three Gorges Bay in China (Liu et al., 2012). Investigators studied the Xiangxi Bay of the Three Gorges Bay and suggested that blooms of blue-green algae, i.e. cyanobacteria, could be prevented from appearing during summer months by keeping $Z_{eu}/Z_{mix,}$ where Z_{eu} and Z_{mix} are the depths of the euphotic and mixing zone, respectively, under a certain threshold value. Because Z_{eu} does not change much during the year, this is equivalent to making sure that the mixing depth is sufficiently large.

Short-term controlled fluctuations of the water level in the Three Gorges Reservoir may be an appropriate management strategy to prevent excessive algal growth in Xiangxi Bay. As shown by Liu et al. (2012), an increase in the water level followed by a comparatively rapid decrease will initiate vertical density currents in Xiangxi Bay that will increase the mixing depth, resulting in reduction of the chlorophyll content of the Bay.

Sufficient vertical mixing is important for wastewater outfalls, particularly ocean outfalls from large population centers such as Los Angeles or New York. Adequate vertical mixing will ensure a high degree of dilution of the effluent. This is necessary for minimizing coliform contamination of nearby beaches and any deleterious impact of the effluent plume on aquatic life.

1.5.1 The Radon Method

Application of the advection–diffusion equation, Equation 1.1 in the vertical direction for the water column of a lake gives (Imboden and Emerson, 1978),

$$D_z \frac{\partial^2 c}{\partial z^2} - \lambda_R c = 0 \tag{1.36}$$

where c is the activity of ^{222}Rn per volume unit, dpm/l, and λ_R is the decay constant. Since the half-life of ^{222}Rn is 3.83 d, the decay constant $\lambda_R = 0.181$ d^{-1}. The z-axis has its origin at the sediment–water interface and points up through the water column, and the origin is at the lake bottom.

The solution to Equation 1.36 with $c = c0$ at $z = 0$ and $c \to 0$ for $z \to \infty$ (deep lake) is,

$$c(z) = c_0 \mathrm{e}^{-\alpha z};\ \alpha = \sqrt{\frac{\lambda_R}{D_z}} \tag{1.37}$$

Thus, from a plot of log z vs. z the slope $-\alpha$, from which D_z may be determined, can be derived. Typical values of D_z for a Swiss lake were 0.05–0.57 cm^2/s (Imboden and Emerson, 1978).

1.5.2 The Tritium–helium-3 Method

This method is based on tritium ($T_{1/2} = 12.33$ yr) from bomb fallout (Torgerson et al., 1977). Tritium decays to helium-3 by emission of β particles,

$$^{3}_{1}\mathrm{H} \xrightarrow[\beta^-]{} {}^{3}_{2}\mathrm{He} \tag{1.38}$$

The helium-3 will then be present in excess levels relative to the amount that is in equilibrium with natural atmospheric helium-3, i.e. 0.00014% of 5.2 ppm. The amount of excess helium-3 relative to the tritium content is a measure of how long the water mass has been isolated from gas exchange with the atmosphere. Gas exchange is maximal during the spring and fall overturns. Build-up of helium-3 from tritium decay occurs during the winter under ice cover, or during summer when lake stratification is maximal and the thermocline presents an effective barrier to gas exchange.

The tritium–helium-3 method may be used to estimate water mass ages and vertical diffusivities. The following definitions apply,

$$\Delta\ 4\mathrm{He}\ (\%) = \left[\frac{\left(^{4}\mathrm{He}\right)_{\mathrm{meas}}}{(^{4}\mathrm{He})_{\mathrm{sat}}} - 1\right] * 100\% \tag{1.39a}$$

$$\delta^{3}\mathrm{He}(\%) = \left[\frac{\left(^{3}\mathrm{He} : {}^{4}\mathrm{He}\right)_{\mathrm{meas}}}{(^{3}\mathrm{He} : {}^{4}\mathrm{He})_{\mathrm{atm}}} - 1\right] * 100\% \tag{1.39b}$$

where $\Delta\ ^{4}\mathrm{He}$ is the $^{4}\mathrm{He}_{\mathrm{excess}}$, $\delta\ ^{3}\mathrm{He}$ is the $^{3}\mathrm{He}$ excess and $^{4}\mathrm{He}_{\mathrm{meas}}$, $^{4}\mathrm{He}_{\mathrm{sat}}$, and $^{4}\mathrm{He}_{\mathrm{atm}}$ are measured, saturation, and atmospheric values of $^{4}\mathrm{He}$ contents respectively. The ratios in Equations 1.39a and 1.39b are determined by mass spectrometry.

The water mass age t is the minimum time since water mass has exchanged gases with the atmosphere and it is determined from,

$$t = \frac{\ln\left[\dfrac{^{3}\mathrm{He}_{\mathrm{excess}}}{\tau} + 1\right]}{\lambda} \tag{1.40}$$

where

$\mathrm{He}_{\mathrm{excess}}$ = the atoms/g $^{3}\mathrm{He}$ over the saturation value,
τ = atoms/g tritium content, and
λ = decay constant of tritium (0.05654 yr^{-1}).

For $t < 1$ yr, Equation 1.40 may be approximated with,

$$t = \frac{1}{\lambda}\frac{^{3}\mathrm{He}_{\mathrm{excess}}}{\tau}, \tag{1.41}$$

or,

$$t = \frac{1}{0.002756}\frac{y}{T}(\delta + 1.4) \quad \text{(days)} \tag{1.42}$$

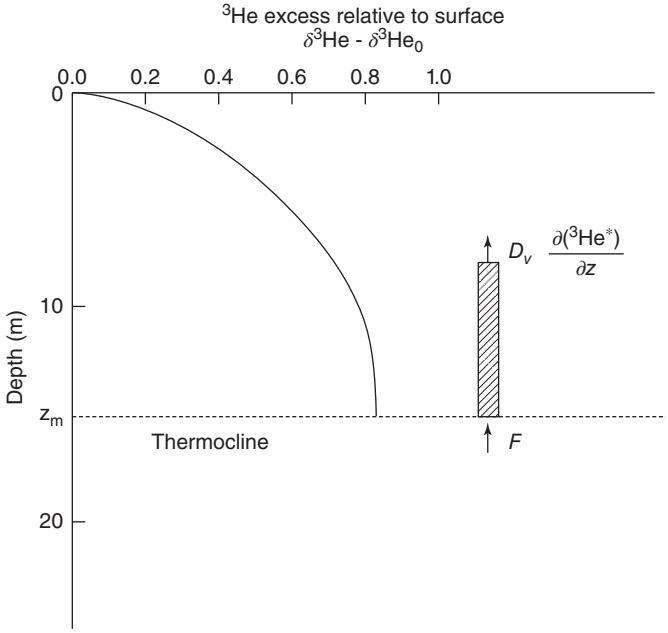

Figure 1.8. ^{3}He buildup and diffusion in the epilimnion of a lake. The graph shows $\delta\ ^3$He–$\delta\ ^3$ He$_0$ % vs. depth. The curve is approximate for Lake Huron, August 1975 with $z_m \sim 17$ m, $D_v \sim 13$ m^2/d. (Source: Adapted from Torgerson et al. (1977))

where

$y =$ ^{4}He content (10^{-8} cc g^{-1} STP)

$T =$ tritium content in tritium units (1 tritium unit = a tritium atom per 10^{18} hydrogen atoms).

Torgerson et al. (1977) found water mass ages ranging from 75 days for Lake Huron up to 150 days for Lake Ontario. A deeper sample generally gives a higher water mass age.

The vertical diffusivity D_v may be derived from the profile of helium-3 vs. depth (Figure 1.8). This profile follows a parabolic curve, as may be seen from a box model for ^{3}He in a layer bounded at the bottom by the thermocline, and the top by a given z-value:

$$\frac{\partial[^3He^*]}{\partial t} = A_0 + D_v \frac{\partial^2[^3He^*]}{\partial z^2} \tag{1.43}$$

where

$[^3He^*] = [^3He] - [^3He]_{solubility}$,

$A_0 = \lambda T$ is the production rate for ^{3}He, i.e. No. of ^{3}He atoms generated by tritium decay per cm^3 per second, and

$\tau =$ tritium concentration, No. of tritium atoms per cm^3.

Assuming steady-state and the following boundary conditions,

$$D_v \frac{\partial[^3\mathrm{He}^*]}{\partial z} = A_0(z_m - z) + F \text{ at depth } z,$$

where z_m is the depth of the box at the thermocline, F is the input flux to the box, and,

$$[^3\mathrm{He}^*] = [^3\mathrm{He}^*]_0 \text{ at } z = 0 \text{ (water surface)},$$

we obtain the solution,

$$[^3\mathrm{He}^*] = [^3\mathrm{He}^*]_0 + \left(\frac{A_0 z_m + F}{D_v}\right) z - \frac{A_0}{2D_v} z^2. \tag{1.44}$$

When the thermocline is present, it presents an effective barrier to ^{3}He flux such that $F = 0$. This solution is shown in Figure 1.8 in units of $\delta\ ^3\mathrm{He} - \delta\ ^3\mathrm{H}_0$ vs. depth where $\delta\ ^3\mathrm{He}_0$ is the $\delta\ ^3$He value at the surface. By fitting measured values of excess helium-3 vs. depth to the model Equation 1.44, it is possible to estimate the vertical diffusivity. Torgerson et al. (1977) found values of D_v ranging from 0.45 cm^2/s for Lake Erie to 1.56 cm^2/s for Lake Huron and 2.93 cm^2/s for Lake Ontario during the season of stratification, i.e. summer and early fall.

The tritium–helium-3 method can also be used to estimate groundwater age, which is important for recharge rates, groundwater residence times, and the calibration of flow models. However, because the aqueous phase molecular diffusion coefficient for ^{3}He is 3.6–5 times that of ^{3}H, the method can give misleading results if it is used for a dual-domain aquifer. For aquitards where diffusive mass transfer is the main transport mechanism, the tritium–helium-3 ages are likely to be artificially raised because of the slower dispersion of ^{3}H. Conversely, for a stream tube, i.e. preferential flow path in a higher conductivity aquifer, the estimated ages can be artificially lowered as a result of the preferential loss of ^{3}He by diffusion out of the tube (LaBolle et al., 2006; Neumann et al., 2008).

Neumann et al. (2008) conducted simulations of the effects of mobile–immobile domain mass transfer on the tritium–helium-3 dating method by considering the transport along stream tubes. They confirmed results of field experiments from the literature, and concluded that the tritium–helium-3 age is difficult to interpret when mass transfer is on the same time scale as the half-life of tritium and the time since the tritium peak was introduced; about 50 yrs.

1.5.3 Evaluation of Mixing Based on Density Gradients

The vertical diffusion coefficient D_z may also be estimated from the density gradient. Thibodeaux (1979) gave the following expression for D_z,

$$D_z = \frac{10^{-4}}{\left|\frac{1}{\rho}\frac{\partial \rho}{\partial z}\right|}, \tag{1.45}$$

which is valid within an order of magnitude. Here the depth z is in m and D_z in cm^2/s. For example, for $1/\rho(\partial\rho/\partial z) = 10^{-5}\ \mathrm{m}^{-1}$, which can be due to a temperature difference of about 2°C over 50 m in a coastal area (National Research Council, 1993), we obtain $D_z = 10\ \mathrm{cm}^2/\mathrm{s}$.

For a submarine outfall, National Research Council (1993) gives the following equations for the maximum rise height of the plume $h_{\max}$ (m) and initial dilution S,

$$h_{\max} = 2.84 \frac{q^{1/3}\left(\dfrac{g\Delta\rho}{\rho}\right)^{1/3}}{\left(\dfrac{-g}{\rho_a}\dfrac{\partial\rho_a}{\partial z}\right)^{1/2}} \tag{1.46}$$

and,

$$S = \frac{0.31\left(\dfrac{g\Delta\rho}{\rho}\right)^{1/3} h_{\max}}{q^{2/3}} \tag{1.47}$$

where

q = discharge rate per unit length of diffuser, $\mathrm{m}^3/(\mathrm{m\ s})$,
g = acceleration as a result of gravity = $9.81\ \mathrm{m/s}^2$,
$\frac{\Delta\rho}{\rho}$ = relative density difference between effluent and receiving water, and
$\frac{\partial\rho_a}{\partial z}$ = average ambient density gradient.

Consider a typical large discharge diffuser with a flow of $5\ \mathrm{m}^3/\mathrm{s}$ (114 mg d), located in 60 m water depth, 10 km offshore. The z axis is vertical. With a 1 km long diffuser, a relative density difference $\Delta\rho/\rho = 0.027$ and an ambient density gradient $(-1/\rho_a)\partial\rho_a/\partial Z = 10^{-5}\ \mathrm{m}^{-1}$, we obtain $h_{\max} = 31$ m and $S = 211$. For increased stratification, the ambient density gradient increases, reducing the plume rise and the dilution.

1.6 HYDRODYNAMIC MODELS

In order to implement an advection–diffusion equation such as Equation 1.1 for dispersion of pollutants in the coastal ocean or lakes, knowledge of the velocity field is required. The temperature and salinity profiles are also needed.

Blumberg and Mellor (1987) developed a three-dimensional hydrodynamic model to predict these variables on the basis of the water continuity equation and the Reynolds version of the Navier–Stokes equation for conservation of momentum, and conservation equations for temperature and salinity. The Earth's rotation is taken into account through the Coriolis effect. This model, with later improvements, is often referred to as the Princeton ocean model. Boundary conditions for the Reynolds equation include known surface wind stress and associated friction velocity. The friction stress and frictional velocity at the bottom must be specified.

The temperature and salinity at boundaries are derived from climatology. Known inflow and outflow determine open boundary conditions. The equations were solved by finite differences, and produced circulation predictions that were quite realistic when compared to available data.

The Princeton model was used to predict water circulation and mixing for the New York Harbor complex, Long Island Sound, and the New York Bight, with a variety of water-forcing as a result of wind, tides, and freshwater inflows in an area with varying topography (Blumberg et al., 1999). A major objective was to improve water quality management. The authors considered two 12-month periods; one from October 1988 to September 1989 for model calibration, and a second from October 1994 to September 1995 for model validation. The grid was based on an orthogonal curvilinear coordinate system. The model differs from most previous models in that it includes large-scale phenomena over annual cycles. On the basis of comparisons of results from an extensive monitoring program, it was found that the model was able to produce elevations and currents with fewer than 10% and 15% errors respectively, on time scales ranging from semidiurnal to annual.

The model was also used to estimate the effects of relocating sewage effluent from Boston Harbor to a new sewage discharge site 14 km offshore in Massachusetts Bay in a water depth of 30 m (Signell et al., 2000). The relocation occurred in year 2000. Predicted variables included effluent dilution, salinity, and circulation.

The simulations demonstrated an overall reduction in the anthropogenic impact on the marine environment following relocation of the outfall to Massachusetts Bay. Effluent levels in the Harbor dropped by a factor of 10 from 1–2% to 0.1–0.2%. Effluent concentrations only exceeded 0.5% within a few kilometer from the new outfall. During summer stratification, effluent released at the sea bed rises and is trapped beneath the pycnocline, i.e. the zone where the water density profile changes rapidly, limiting the local increase in effluent concentration to the lower layer; whereas surface concentrations decrease relative to the harbor outfall.

Liu et al. (2006) provided an example in which the Princeton model was applied to a freshwater environment. They considered a nearshore finite element transport model for fecal pollution in Lake Michigan. The model included a water continuity equation and a vertically integrated version of the momentum conservation equation. Coupled to this, the model included an advection–diffusion equation for the transport of *Escherichia coli*, *Enterococci*, and temperature. The latter equation included a source or sink term for temperature reflecting shortwave radiation, long wave back radiation, condensation, and heat flux from sensible heat transfer and heat inputs from tributaries.

The model produced good agreement between observed and simulated bacteria concentration at Mt. Baldy Beach, Indiana, except on Julian day 218, 2004, one of 3 days when the *esp* human pollution indicator was found. This suggested that there was a significant input of fecal contamination that did not come from Trail Creek or Kintzele Ditch. It was concluded that sunlight causes inactivation of bacteria in the surf-zone, and that sunlight, temperature, and sedimentation provide a better description of inactivation than first-order kinetics.

Hydrologic models can be adapted to simulate pathogen fate and transport as demonstrated by Dorner et al. (2006) for Canagagigue Creek, Ontario, Canada. The authors used an existing hydrologic model, WATFLOOD, that had been previously calibrated for the Grand River Watershed including Canagagiaue Creek. The model underwent revised calibration because of the inclusion of tile drainage and a smaller grid size. Several waterborne pathogens were considered: *Cryptosporidium* spp. *Giardia* spp., *Campylobacter* spp. and *E. coli* O157:H7. Calibration was carried out for *E. coli* by trial and error following calibration of the hydrologic model.

Application of the model to the pathogen *E. coli* O157:H7 produced results within about one order of magnitude of the observed data. The sparsity of pathogen data presents a challenge for model testing and prediction. The authors observed a rapid increase in measured *E. coli* concentrations during storm events, suggesting that re-suspended sediments can contribute significantly to measured bacteria concentrations.

1.7 GROUNDWATER PLUMES

Application of Equation 2.1 to a one-dimensional groundwater system with reaction gives,

$$\frac{\partial c}{\partial t} = D\frac{\partial^2 c}{\partial x^2} - \upsilon\frac{\partial c}{\partial x} - r \tag{1.48}$$

where

c = concentration of a pollutant, $\mu g/cm^3$, and
r = rate of which the pollutant is removed, $\mu g/(cm^3\ s)$.

In the case where there is partitioning of a chemical between the aqueous and soil phase,

$$s = K_d c \tag{1.49}$$

where

s = pollutant concentration per mass unit of solids, $\mu g/g$, and
c = pollutant concentration in the aqueous phase, $\mu g/cm^3$.

Thus, the unit of the partition coefficient K is pore volume per mass unit of solids, cm^3/g. The left hand side of Equation 1.48 becomes,

$$\varphi\frac{\partial c}{\partial t} + (1-\varphi)\rho_s K_d\frac{\partial c}{\partial t} \tag{1.50}$$

where ϕ is the porosity, ρ_s is the solids density, g/cm^3, and c is the pollutant concentration in the aqueous phase. Introducing the bulk sediment density, g/cm^3, $\rho = (1-\phi)\rho_s$, Equation 1.48 is transformed into:

$$\left(1 + \frac{\rho K_d}{\varphi}\right)\frac{\partial c}{\partial t} = \frac{1}{\varphi}\left(D\frac{\partial^2 c}{\partial x^2} - \upsilon\frac{\partial c}{\partial x} - r\right) \tag{1.51}$$

The right hand side refers to the system of water and soil. In this system, pollutant transport occurs only in the aqueous phase because the aquifer material is stationary. Assuming that degradation, r, only takes place in the aqueous phase, we obtain:

$$\frac{\partial c}{\partial t} = \frac{D}{1+R}\frac{\partial^2 c}{\partial x^2} - \frac{v}{1+R}\frac{\partial c}{\partial x} - \frac{k_d}{1+R} \tag{1.52}$$

where

c = pollutant concentration in the aqueous phase, $\mu g/cm^3$,
v = pore water velocity, cm/s,
k_d = reaction rate in the aqueous phase = r/ϕ, $\mu g/(cm^3 s)$, and
R = retardation = $(\rho\ K_d)/\phi$.

Equation 1.52 has the same form as Equation 1.1 except that diffusivity, velocity, and reaction rate have been multiplied with the retardation factor, $R.F. = 1/(1+R)$. Thus, solutions such as Equation 1.27 for a pulse or Equations 1.31 and 1.32 for a step function without reaction, apply to the above case when D and v are multiplied with the appropriate retardation factor. It may be shown that the retardation factor is equal to the mass of the pollutant in the mobile phase divided by the total mass of the pollutant. From Equation 1.52 it can be seen that *R.F.* can also be expressed as,

$$R.F. = \frac{v_p}{v}, \tag{1.53}$$

where v_p is the velocity of the pollutant ($\leq v$).

High molecular weight compounds that are strongly particle-bound will be slowed down considerably; whereas low molecular weight compounds will experience minimal retardation, and will therefore follow the plume of groundwater with only a small delay. In fact, the groundwater system mimics a gas or liquid chromatograph, providing separation of various compounds according to their partition coefficients between the mobile and stationary phases.

1.8 SEDIMENT MIXING

For sediments, many compounds of interest, e.g. ^{210}Pb, Pb, ^{137}Cs, PAHs, and PCBs, are strongly particle-associated. The sediment particles themselves are mixed by bioturbation or physical action such that only the solid phase becomes of interest, except when the mixing intensity is very small (Robbins et al., 1979; Officer and Lynch, 1989; Christensen and Bhunia, 1986). Sediment mixing is of interest because it can distort historical records of pollutants in sediments, and can provide a means of returning pollutants from the sediments to the water column.

While most early papers recognized just one category of particles participating in the mixing process, Fukumori et al. (1992) found it to be necessary to distinguish between settling ($\geq$ 50 μm) and colloidal ($\geq$ 2 μm) particles. The system of equations

for conservation of pollutant and sediment mass may be written as,

$$-\frac{\partial}{\partial z}(v\rho s) + \frac{\partial}{\partial z}\left(D\frac{\partial \rho s}{\partial z}\right) - \lambda \rho s = \frac{\partial \rho s}{\partial t} \tag{1.54a}$$

$$-\frac{\partial}{\partial z}(\rho v) = \frac{\partial \rho}{\partial t} \tag{1.54b}$$

with boundary conditions,

$$\left.\begin{aligned} \rho s v - D\frac{\partial \rho s}{\partial z} &= J_0(t) \qquad \text{at } z = 0 \\ \frac{\partial \rho s}{\partial z} &= 0 \qquad \text{at } z = l \end{aligned}\right\} \tag{1.55}$$

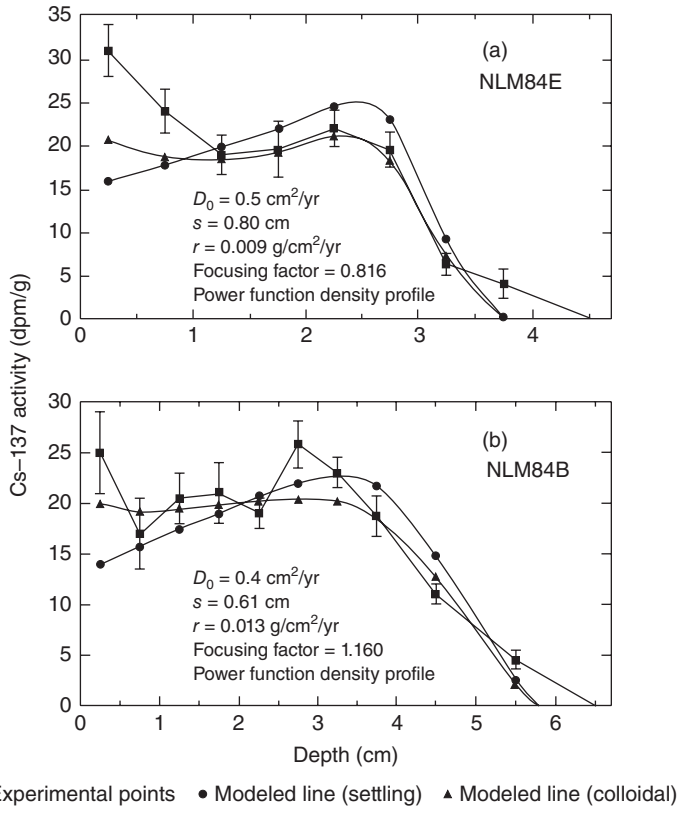

Figure 1.9. Comparison of experimental and calculated ^{137}Cs activities (a) in core NLM84E and (b) in core NLM84B. The calculated curves are from a finite difference method. The calculated curves apply to both the case where ^{137}Cs is associated with settling particles, and to the case where ^{137}Cs is associated with colloidal particles. (Source: Reproduced from Fukumori et al. (1992), with permission from Elsevier.)

where z (cm) is the depth below the sediment-water interface, v (cm/yr) is the burial velocity relative to the interface, t (y) is the time, D (cm^2/yr) is the diffusion coefficient, $\lambda(yr^{-1})$ is the radioactive decay constant, and $\rho = (1 - \phi)\rho_s$ is the bulk density of sediment solids. The porosity is designated ϕ and the solids density $\rho_s = 2.45$ (g/cm^3).

The tracer and bulk solids Equations 1.54a and 1.54b are valid for colloids, e.g. clay particles. For settling particles, the diffusive flux $D\,\partial(\rho s)/\partial z$ should be replaced by $D\,\rho\,\partial s/\partial z$.

As an example of the application of these equations, consider Figure 1.9, which shows measured and calculated values for ^{137}Cs activity in sediments from northern Lake Michigan (Fukumori et al., 1992). Distributions were calculated using a finite difference method under the assumptions that ^{137}Cs is associated with colloidal clay particles, which is known to be the case (Comans et al., 1991; Ab Razak et al., 1996), and the hypothetical case where ^{137}Cs would be bound to larger settling particles. The ^{137}Cs input flux $J_0(t)$ was taken from Health and Safety Laboratory (1977), and the bulk sediment density follows a power function (Fukumori et al., 1992). From Figure 1.9 it is clear that the colloidal interpretation for ^{137}Cs is the more accurate, thus supporting Equations 1.54a and 1.54b. The high ^{137}Cs activity values (dpm/g) near the top of the sediment in this case occur because of the low bulk density ρ in this region. For ^{210}Pb, which is associated with larger particles (Shimp et al., 1971; Ab Razak et al., 1996), the alternate form containing a diffusive flux of $D\,\rho\,\partial s/\partial z$ gives, as expected, better agreement between calculated and experimental activities (see Fukumori et al., 1992).

REFERENCES

Ab Razak, IA, Li, A, Christensen, ER. Association of PAHs, PCBs, ^{137}Cs, and ^{210}Pb with clay, silt, and organic carbon in sediments. *Wat. Sci. Technol.* 1996;34(7–8):29–35.

Blumberg, AF, Mellor, GL. A description of a three-dimensional coastal ocean circulation model. In: Heaps, NS, Editor. *Three dimensional coastal ocean models*. Washington, DC: American Geophysical Union; 1987. p 1–16.

Blumberg, AF, Khan, LA, St. John, JP. Three-dimensional hydrodynamic model of New York Harbor region. *J. Hydr. Eng. ASCE*, 1999;125(8):799–816.

Christensen, ER, Bhunia, PK. Modeling radiotracers in sediments: comparison with observations in Lakes Huron and Michigan. *J. Geophys. Res*. 1986;91(C7):8559–8571.

Christensen, ER, Edgington, DN, Giesy, JP. Contaminated Aquatic Sediments. *Wat. Sci. Technol.* 1993;28(8–9).

Christensen, ER, Karls, JF. Unmixing of lead, ^{137}Cs, and PAH records in lake sediments using curve fitting with first- and second order corrections. *Wat. Res.* 1996;30(11):2543–2558.

Christensen, ER, Phoomiphakdephan, W, Ab Razak, IA. Water quality in Milwaukee, Wisconsin versus intake crib location. *ASCE J. Environ. Eng.* 1997;123(5):492–498.

Comans, RNJ, Haller, M, De Preter, P. Sorption of cesium on illite: nonequilibrium behavior and reversibility. *Geochim. Cosmochim. Acta.* 1991;55:433–440.

Cox, TJ, Runkel, RL. Eulerian-Lagrangian numerical scheme for simulating advection, dispersion and transient storage in streams and a comparison of numerical methods. *J. Environ. Eng. ASCE*, 2008;134(12):996–1005.

Dorner, SM, Anderson, WB, Slawson, RM, Kouwen, N, Huck, PM. Hydrologic modeling of pathogen fate and transport. *Environ. Sci. Technol.* 2006;40(15):4746–4753.

Frieseke, RW, Christensen, ER. Groundwater remediation with granular collection system. *ASCE J. Environ. Eng.* 1995;122(6):546–549.

Fukumori, E, Christensen, ER, Klein, RJ. A model for ^{137}Cs and other tracers in lake sediments considering particle size and the inverse solution. *Earth Planet. Sci. Lett.* 1992;114:85–99.

Gershon, ND, Nir, A. Effects of boundary conditions of models on tracer distributions in flow through porous mediums. *Wat. Res.* 1969;5(4):830–839.

Guinasso, NL Jr., Schink, DR. Quantitative estimates of biological mixing rates in abyssal sediments. *J. Geophys. Res.* 1975;80:3032–3043.

Haas, CN, Vamos, RJ. *Hazardous and Industrial Waste Treatment*. Englewood Cliffs, New Jersey: Prentice Hall; 1995.

Harremoës, P. 1978. Analytical pollution models of well mixed estuaries. In: *Coastal Pollution Control*. *World Health Organization Training Course*, Vol. III, Geneva, Switzerland.

Health and Safety Laboratory. 1977. *Final Tabulation of Sr-90 Fallout Data: 1954-1976, Environ. Quarterly, HASL-329*, Energy Research and Development Admin., New York.

Hou, X, Aldahan, A, Nielsen, SP, Possnert, G, Nies, H, Hedfors, J. Speciation of ^{129}I and ^{127}I in seawater and implications for sources and transport pathways in the North Sea. *Environ. Sci. Technol.* 2007;41(17):5993–5999.

Imboden, DM, Emerson. Natural radon and phosphorus as limnologic tracers: Horizontal and vertical eddy diffusion in Greifensee. *Limnol. Oceanogr.* 1978;23:77–90.

LaBolle, EM, Fogg, GE, Eweis, JB. Diffusive fractionating of ^{3}H and ^{3}He in groundwater and its impact on groundwater age estimates. *Wat. Res.* 2006;42:W07202, doi: 10.1029/2005WR004WR004756.

Lapidus, L, Amundson, NR. Mathematics of adsorption in beds. VI The effect of longitudinal diffusion in ion exchange and chromatographic columns. *J. Phys. Chem.* 1952;56:984–988.

Lawson, R, Anderson, MA. Stratification and mixing in Lake Elsinore, California: An assessment of axial flows for improving water quality in a shallow eutrophic lake. *Wat. Res.* 2007;41:4457–4467.

Lee, YW, Dahab, MF, Bogardi, I. Nitrate-risk assessment using fuzzy-set approach. *ASCE J. Environ. Eng.* 1995;121(3):245–256.

Li, Y, Wang, Y, Pennell, KD, Abriola, LM. Investigation of the transport and deposition of fullerene (C60) nanoparticles in quartz sands under varying flow conditions. *Environ. Sci. Technol.* 2008;42(19):7174–7180.

Liu, L, Liu, D, Johnson, DM, Yi, Z, Huang, Y. Effects of vertical mixing on phytoplankton blooms in Xiangxi Bay of Three Georges Reservoir: Implications for management. *Wat. Res.* 2012;46:2121–2130.

Liu, L, Phanikumar, MS, Molloy, SL, Whitman, RL, Shively, DA, Nevers, MB, Schwab, DJ, Rose, JB. Modeling the transport and inactivation of *E.coli* and Enterococci in the nearshore region of Lake Michigan. *Environ. Sci. Technol.* 2006;40(16):5022–5028.

McQuivey, RS, Keefer, TN. Simple method for predicting dispersion in streams. *ASCE J. Environ. Eng. Div.* 1974;100:997–1011.

Mortimer, CH. *The Lake Michigan Pollution Case. A Review and Commentary on the Limnological and Other Issues*. Milwaukee, Wisconsin: Center for Great Lakes Studies, University of Wisconsin-Milwaukee; 1981.

National Research Council. Managing Wastewater in Coastal Urban Areas. Committee on Wastewater Management for Coastal Urban Areas. Water Science and Technology Board. *Commission on Engineering and Technical Systems*, pp 237–238. Washington, DC: National Academy Press; 1993.

Neumann, RB, Labolle, EM, Harvey, CF. The effects of dual-domain mass transfer on the Tritium-Helium-3 dating method. *Environ. Sci. Technol.* 2008;42(13):4837–4843.

Officer, CB, Lynch, DR. Bioturbation, sedimentation, and sediment-water exchanges. *Estuar. Coast. Shelf Sci.* 1989;28:1–12.

Robbins, JA, McCall, PL, Fisher, JB, Krezoski, JA. Effects of deposit feeders on migration of ^{137}Cs in lake sediments. *Earth Planet. Sci. Lett.* 1979;42:277–287.

Schladow, SG, Fisher, IH. The physical response of temperate lakes to artificial destratification. *Limnol. Oceanogr.* 1995;40(2):359–373.

Shimp, NF, Schleicher, JA, Ruch, RR, Heck, DB, Leland, HV. Trace Element and Organic Carbon Accumulation in the Most Recent Sediments of Southern Lake Michigan. Illinois State Geol. Surv. Environ. Geol. Notes No. 41; 1971.

Signell, RP, Jenter, HL, Blumberg, AF. Predicting the physical effects of relocating Boston's sewage outfall. *Estuar. Coast. Shelf Sci.* 2000;50:59–72.

ter Laak, TL, Van Eijkeren, JCH, Busser, FJM, Van Leeuwen, HP, Hermens, JLM. Facilitated cnd polybrominated diphenyl ethers by dissolved organic matter. *Environ. Sci. Technol.* 2009;43(5):1379–1385.

Thibodeaux, LJ. *Chemodynamics*. New York: John Wiley and Sons, Inc.; 1979.

Torgerson, T, Top, Z, Clarke, WB, Jenkins, WJ, Broecker, WS. A new method for physical limnology - tritium - helium-3 ages - results for Lakes Erie, Huron, and Ontario. *Limn. Oceanogr.* 1977;22(2):181–193.

Weber, WJ Jr, DiGiano, FA. *Process Dynamics in Environmental Systems*. New York: John Wiley and Sons, Inc.; 1996.

Wetzel, RG 1975. *Limnology*. Philadelphia: W.B. Saunders Company.